Oxoammonium-Catalyzed Oxidation of *N*-Substituted Amines

Jonas Rein,[1,‡] Bartosz Górski,[1,‡] Yukun Cheng,[1,†] Zhen Lei,[2,†] Frederic Buono,[2] and Song Lin[1,*]

[1]Department of Chemistry and Chemical Biology, Cornell University, Ithaca, New York 14853, United States.

[2]Chemical Development U.S., Boehringer Ingelheim Pharmaceuticals, Inc., 900 Ridgebury Rd, Ridgefield, CT 06877, United States

ABSTRACT: We report the development of oxoammonium-catalyzed oxidation of *N*-substituted amines *via* a hydride transfer mechanism. Steric and electronic tuning of catalyst led to complementary sets of conditions that can oxidize a broad scope of carbamates, sulfonamides, ureas, and amides into the corresponding imides. The reaction was further demonstrated on a 100-g scale using a continuous flow setup.

The oxidation of *N*-substituted amines to their corresponding amides is a highly useful transformation.[1–11] For example, it has been used to synthesize *N*-carbamoyl lactams, which are key intermediates in numerous total syntheses and pharmaceutical manufacturing processes (Scheme 1B).[3–9] While related amine functionalizations have been developed to introduce a single α-substituent by means of transition-metal catalysis, photocatalytic hydrogen atom transfer (HAT),[12–14] and Shono-type electrolysis,[15,16] methodologies for the direct oxidation of both geminal α-C–H bonds to a carbonyl remain scarce. In fact, a survey of pharmaceutical patents for the oxidation of carbamates, ureas, or amides revealed that over 80%[17] of examples employ Ru catalysts in combination with $NaIO_4$ or $NaBrO_3$ (Scheme 1A).[1,2] The reliance on an expensive noble metal and the generation of highly toxic and volatile RuO_4 as the active intermediate may reduce the safety, practicality, and scalability of this approach. Other methods using strong inorganic oxidants such as $KMnO_4$ or CrO_3 suffer from limited substrate generality and functional group compatibility. Recently, White *et al.* pioneered the use of non-heme Mn and Fe complexes for the late-stage hydroxylation of amine derivatives via metal-oxo-mediated HAT.[18–20] While the carbonyl product could also be obtained in some cases, the method has been predominantly used for the functionalization of sulfonamides and amides and has not been demonstrated for amide with common *N*-protecting groups such as Boc, Cbz, and Fmoc.[20]

In a seminal contribution, Stahl developed the electrochemical oxidation of cyclic carbamates mediated by 40–60 mol% ketoABNO (Scheme 1C).[21] The aminoxyl radical is oxidized to the corresponding oxoammonium ion that serves as a potent hydride acceptor, formally abstracting a H^- from a hydridic α-C–H bond.[22–28] The methodology was later further developed by Merck for the oxidation of an Orexin receptor agonist fragment.[29,30] However, this approach required high mediator loadings due to the formation of an inert aminoxyl-substrate adduct upon hydride abstraction **1**. Further, it could not currently be extended to the oxidation of sulfonamides and amides.

Scheme 1. Background and introduction.

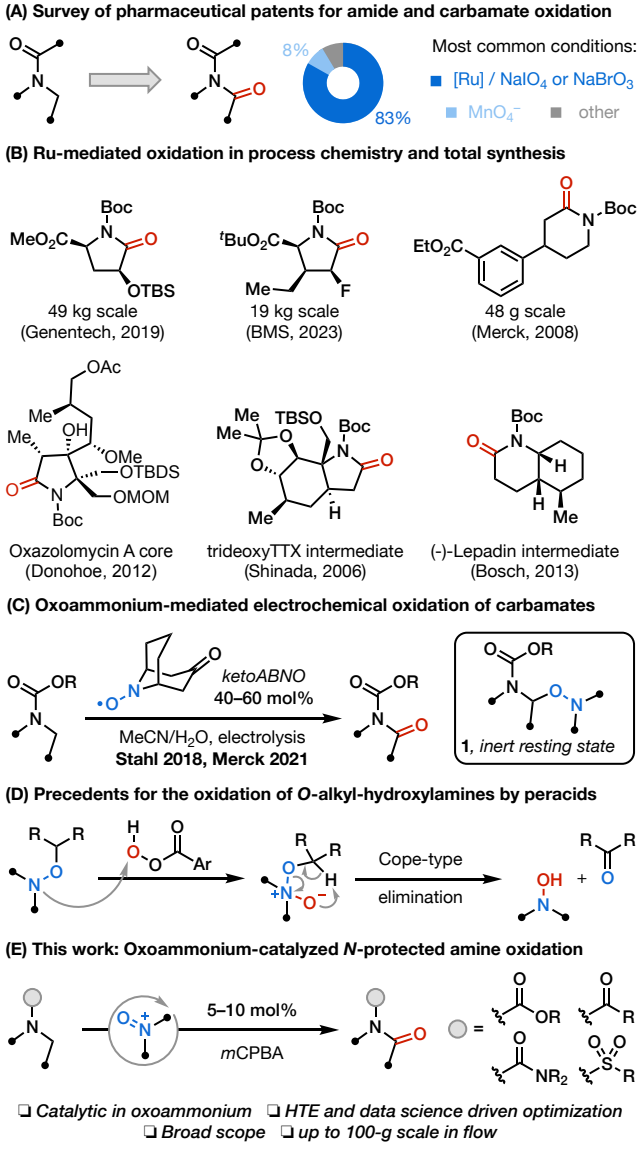

We aim to achieve the oxidation of a broader range of amine derivatives (including carbamates, sulfonamides, ureas, and

https://doi.org/10.26434/chemrxiv-2024-brd62 **ORCID:** https://orcid.org/0000-0001-8237-6519 Content not peer-reviewed by ChemRxiv. **License:** CC BY-NC 4.0

amides) using a catalytic amount of aminoxyl. To achieve catalytic turnover, we sought inspiration from the literature, which showed that alkoxyamines analogous to **1** can undergo oxidation to ketones upon exposure to peracids (Scheme 1D).[31–33] This reaction proceeds first through O-atom transfer to the alkoxyamine to form an *N*-oxide followed by a Cope-type elimination to forge the carbonyl group. We aimed to leverage this reactivity to activate the otherwise inert catalyst resting state (**1**). Indeed, adduct **3** prepared from *N*-tosylpyrrolidine and ketoABNO^{+}SbF$_6^{-}$ rapidly reacted with *meta*-chloroperoxybenzoic acid (*m*CPBA), resulting in quantitative formation of product **4** (Scheme 2A). This reactivity thus provides the missing piece of the envisioned catalytic cycle (Scheme 2B). The catalysis begins with hydride transfer from substrate **2** to the oxoammonium form of the catalyst (**I**), and the resultant hydroxylamine **III** and iminium ion **II** recombine to generate adduct **IV**. **IV** undergoes reaction with *m*CPBA followed by Cope elimination, which conveniently furnishes the desired amide product and releases hydroxylamine **III**. This intermediate is oxidized to the oxoammonium ion to close the catalytic cycle.

Scheme 2. Establishing catalytic turnover.

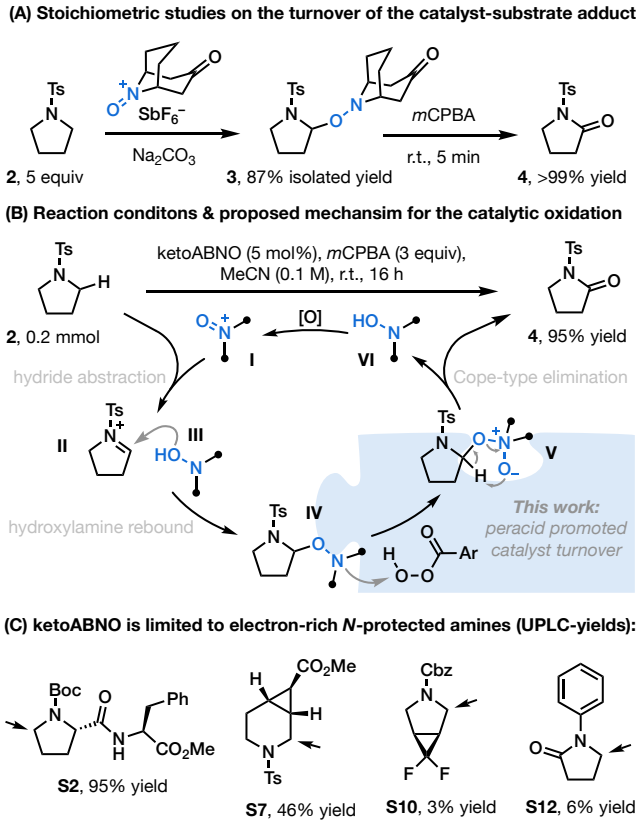

Under this hypothesis, we found that using *m*CPBA as the terminal oxidant, the oxidation of pyrrolidine **2** readily took place in MeCN, providing *N*-protected amide **4** in up to 95% yield with only 5 mol% of ketoABNO (Scheme 2B). With the mechanistic basis for catalyst turnover established, we surveyed an initial scope of amine derivatives (Scheme 2C). While high yields were obtained for carbamate **S2**, substantially lower conversion was observed for more electron-poor substrates including sulfonamide **S7**, carbamate **S10**, and amide **S12**.

To broaden the scope of this method, we first carried out experimental and computational studies to elucidate catalyst structural features that influence the rate of hydride abstraction. We assembled a library of known aminoxyl radicals (**A1**–**A14**) and analyzed the steric and electronic properties of their oxoammonium ions (Figure 1B, compounds in black). The electronic property of the catalysts was reflected by their reduction potentials (E_{red}) determined using cyclic voltammetry (CV).[34,35] The reversibility of the voltammogram also allowed us to directly assess the stability of the oxoammonium ion, with a fully reversible peak indicating that the oxoammonium is stable on the voltammetry timescale (i.e., > 3 seconds). The steric accessibility of the oxoammonium reactive site (O=N^{+}) was assessed by the percent buried volume (%V_{bur}), quantifying the percentage of space occupied by the catalyst backbone within a sphere of radius 2.5 Å centered around the oxygen atom (Figure 1A).[36,37] With these two parameters, a stereoelectronic map was created for the collection of catalysts, revealing that there exist very few stable oxoammonium ions in the literature that are both highly oxidizing and unhindered (upper left corner).[38–41] To address this limitation, we designed and prepared eight new aminoxyl radicals (**A15–A22**, Figure 1A, compounds in blue). In particular, AzcF^{+} (oxidized form of **A21**) represents the most oxidizing stable oxoammonium ion reported to date.

We then assembled a scope of 12 *N*-protected amines including carbamates, sulfonamides, amides, and a urea, featuring various ring sizes and structures that are often encountered in bioactive molecules (**S1–S12**). Through high-throughput experimentation using 384-well plates, we rapidly surveyed all catalyst-substrate combinations in two different solvents, dichloroethane and acetonitrile. Further, each system was investigated with and without an acid co-catalyst, $HNTf_2$, which was found to improve catalyst turnover in a parallel project in our laboratory on the development of oxoammonium-catalyzed ether oxidations.[42,43]

Analysis of the full dataset (1056 reactions) allowed us to categorize all catalysts into four regions on the stereoelectronic map based on the observed reactivity (Figure 1A). Region 1 encompasses highly oxidizing, unhindered catalysts, which allowed for the activation of the most challenging substrates including amides, which showed low conversion with any other catalysts. Region 2 includes unhindered catalysts with moderate reduction potentials (291–529 mV) and are optimal for the oxidation of sulfonamides and carbamates with high yields and clean reaction profiles. Region 3 includes unhindered catalysts with low reduction potentials (≤ 204 mV), which selectively reacted with *N*-Boc pyrrolidines **S2**/**S3** and urea **S1** in moderate yields. Region 4 contains mostly sterically hindered aminoxyls, which are universally ineffective catalysts regardless of reduction potential, in addition to poorly oxidizing **A8**. While the majority of these aminoxyls display reversible CV behaviors, three species (**A6**, **A15**, **A18**) showed irreversible oxidation waves and did not provide catalytic reactivity. This reactivity map shows that both steric and electronic factors must be considered to predict the hydride accepting tendency of oxoammonium ions.

https://doi.org/10.26434/chemrxiv-2024-brd62 **ORCID:** https://orcid.org/0000-0001-8237-6519 Content not peer-reviewed by ChemRxiv. **License:** CC BY-NC 4.0

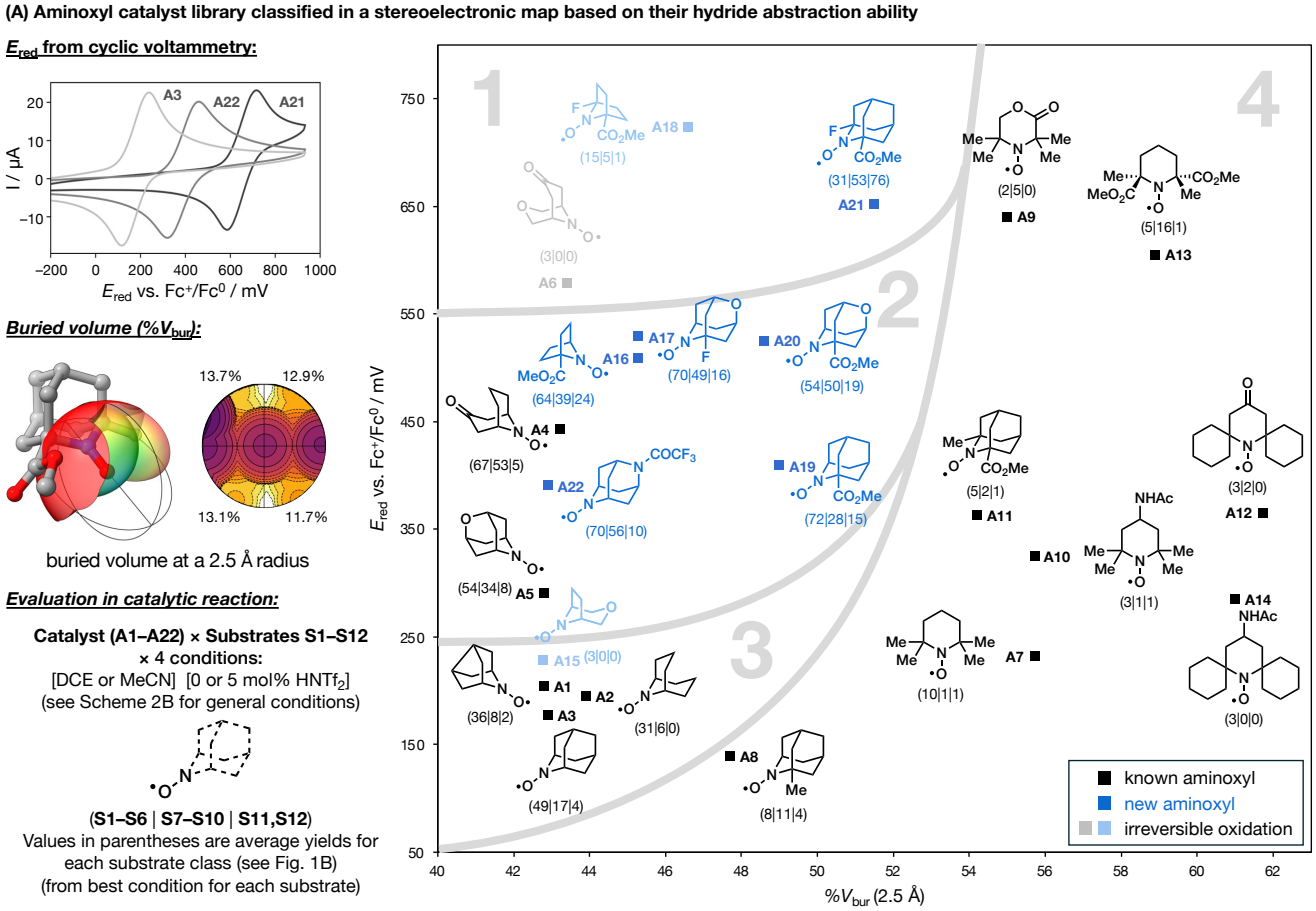

Figure 1. (A) Aminoxyl catalyst library and a stereoelectronic reactivity map based on reduction potential and percent buried volume (see SI for details). (B) Identification of three complementary sets of optimal reaction conditions via high-throughput screening (2.5 µmol substrate, 0.05 M concentration, 16 h, r.t.).

https://doi.org/10.26434/chemrxiv-2024-brd62 **ORCID:** https://orcid.org/0000-0001-8237-6519 Content not peer-reviewed by ChemRxiv. **License:** CC BY-NC 4.0

Wholistically, these experiments reveal intricate catalyst-substrate dependencies with no singular system delivering satisfactory yields for all substrates. Nevertheless, we identified three complementary sets of reaction conditions (Condition A–C) (Figure 1B) that provided reactivity coverage of the entire screening panel, using a python script that ranked all ternary condition combinations based on the highest average yield when the best of three conditions is used for each substrate (see SI). Condition A uses commercially available ketoABNO catalyst (**A4**) in MeCN solvent. Condition B employs TFAZADO (**A22**) with 2.5 mol% $HNTf_2$ additive in DCE solvent. These two catalysts occupy a similar region on the stereoelectronic map and largely exhibit the same substrate coverage, providing reactivity for most carbamates and sulfonamides without strongly deactivating groups. In the HTE screening, we found that DCE is a superior solvent over MeCN,[44] which allowed for more electron-deficient substrates such as *N*-nosylpyrrolidine **S8** to be oxidized in good yield. However, ketoABNO is incompatible with DCE as it readily deactivates through the Baeyer-Villiger reaction, and the use of TFAZADO is thus necessary in Condition B.

Condition C uses highly oxidizing AzcF (**A21**) with 2.5 mol% $HNTf_2$ in DCE, which unlocks the oxidation of amides (**S11**, **S12**) and substrates bearing strong inductively withdrawing substituents (e.g., **S10**). However, Condition C provided diminished yields for more electron-rich substrates (**S1**–**S6**). Hemiaminal side products were observed from addition of *m*-chlorobenzoate (*m*CBA, byproduct formed from *m*CPBA) to the iminium intermediates. We attribute this undesired reactivity to the inefficient formation of the substrate-catalyst adduct (**II** + **III** → **IV** in Scheme 2) due to the poor nucleophilicity of AzcF-derived hydroxylamine and the comparatively low electrophilicity of the iminium ions of electron-rich carbamates and ureas.

Using the optimal conditions, we then explored the synthetic utility of the method (Scheme 3). We first performed further reaction optimization and sensitivity study at a 0.2-mmol preparative scale, showing that the protocol is insensitive to the presence of air, moisture, and variations in reaction scale and concentration. For carbamates, sulfonamides, and ureas, both Conditions A and B were investigated, and results from the higher yielding condition are presented. The substrates that gave poor yields in the above experiments, in addition to the most challenging amide substrates, were subjected to Condition C. Various *N*-substituted pyrrolidines (**5**–**10**), piperidines (**11**–**14**), azepanes (**15**, **16**), fused bicycles (**17**–**20**), a morpholine (**21**), and an acyclic amine (**22**) were cleanly converted to their corresponding imides using Condition A. Notably, the α-C–H oxidation (with 5 mol% catalyst) outcompeted olefin epoxidation in vinyl bromide **13** and allyl-β-homoproline **10**, as well as Baeyer-Villiger oxidation of ketone **17**. Condition B proved to be competent for the oxidation of Boc- and Fmoc- protected proline derivatives (**23**–**26**), a dipeptide (**27**), a nosyl-protected pyrrolidine (**28**), and fused and bridged biheterocycles (**29**– **31**). Notably, we are able to obtain oxidized *trans*-*L*-3-hydroxyproline **25** in 70% yield, providing an alternative to the ruthenium-mediated oxidation that has been applied in the total synthesis of (+)-Febrifugine,[45] (-)-Securinine,[46] (-)-Allosecurinine,[47] and Teixobactin.[48]

Finally, Condition C enabled the oxidation of *gem*-difluorocyclopropyl-substituted carbamate **32** and Cbz-Fluoxetine **34**, as well as the oxidative fragmentation of bridged bicycle **35**. AzcF's ability to activate amides (**33**, **36**–**41**), a ubiquitous motif in pharmaceuticals and bioactive molecules, enabled the selective oxidation of Asenapine (**38**) and Ibuprofen (**39**) derivatives, as well as Noopet (**40**) and Levetiracetam (**41**). To address the competitive oxygenation of basic nitrogen-containing functional groups by *m*CPBA, we employed trifluoroacetic acid to achieve transient protection,[16] which allowed pyridine **42** to be obtained in 50% yield.[49]

This hydride transfer-mediated method shows complementary selectivity to radical-based C–H functionalization reactions. Indeed, various substrates studied herein contain weak benzylic (**6**, **11**, **14**, **34**, **38**–**40**), allylic (**10**, **13**), and doubly benzylic (Fmoc in **26**) C–H bonds, which are susceptible to HAT,[50] underwent selective amine α-oxidation. Further, functionalities that are sensitive to oxidation in Shono-type electrolysis[21] and RuO_4-mediated methods[51] such as benzylic C–H bonds, electron-rich arenes, and olefins are tolerated.

https://doi.org/10.26434/chemrxiv-2024-brd62 **ORCID:** https://orcid.org/0000-0001-8237-6519 Content not peer-reviewed by ChemRxiv. **License:** CC BY-NC 4.0

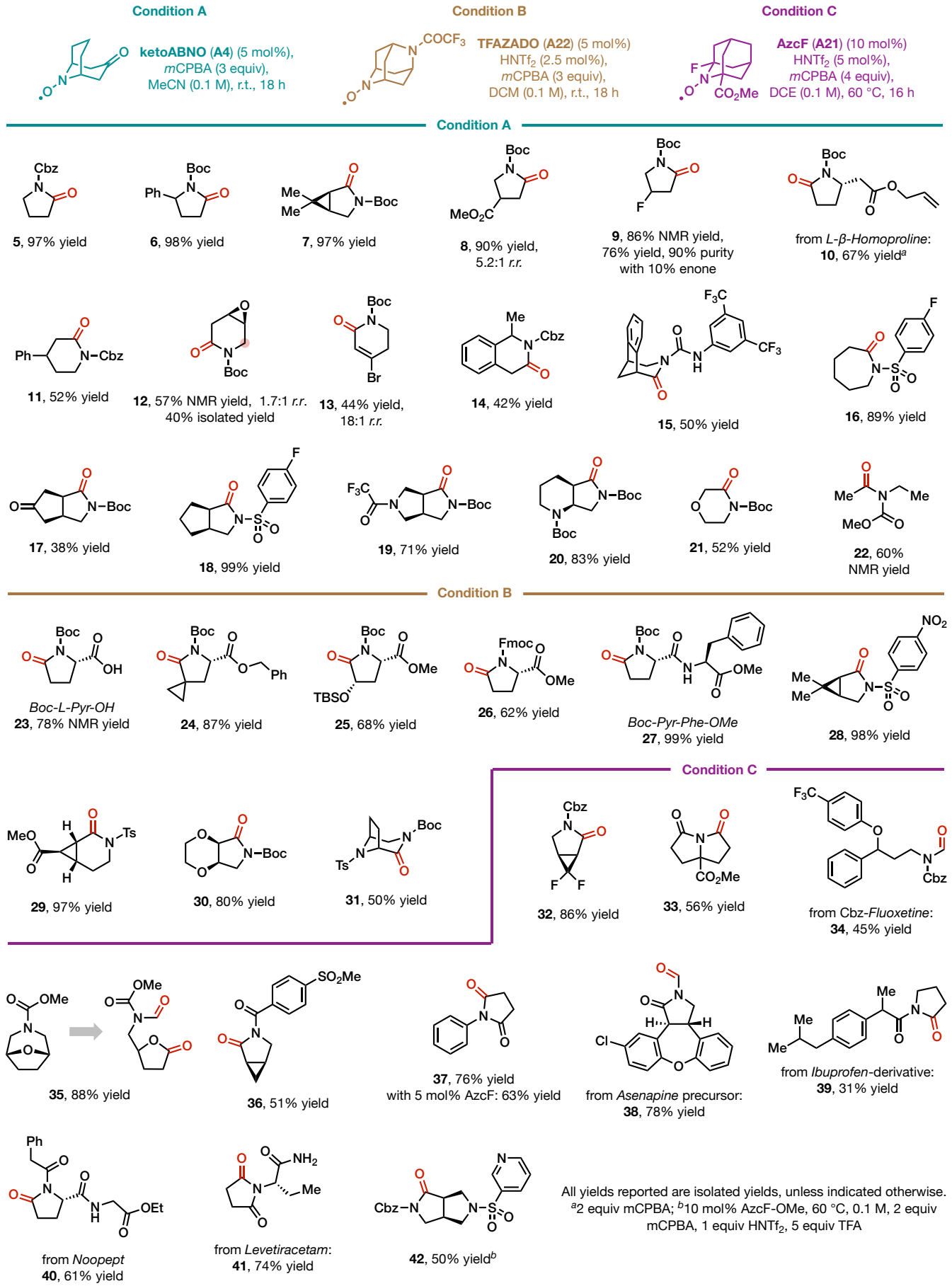

Scheme 3. Substrate Scope

https://doi.org/10.26434/chemrxiv-2024-brd62 **ORCID:** https://orcid.org/0000-0001-8237-6519 Content not peer-reviewed by ChemRxiv. **License:** CC BY-NC 4.0

(A) Schematic reaction setup for the 100-g scale, 10-hour continuous flow scale-up with inline FT-IR analysis

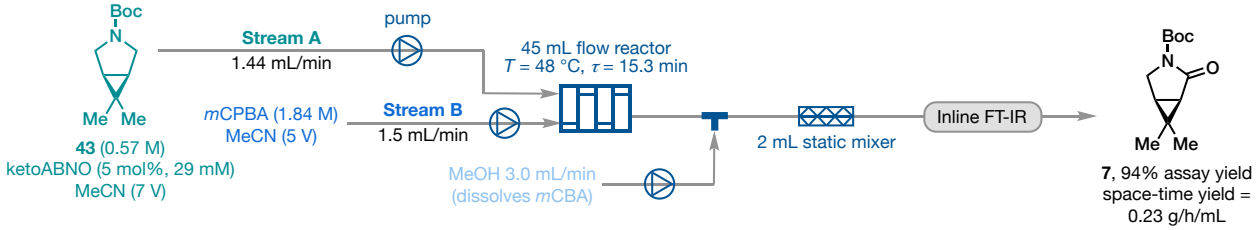

(B) Optimization of the flow reaction conditions

Entry	Flow Rate **A** [mL/min]	τ [min]	T [°C]	Mixer	Conversion [%]	Yield [%]
1	1.44	15	36	Tee	65	65
2	1.44	15	42	Tee	86	85
3	1.44	15	48	Tee	93	88
4	1.44	15	56	Tee	98	85
5	2.25 **A** = **B**	10	56	Tee	82	71
6	**1.44**	**15**	**48**	**Tee + static**[a]	**>99**	**94**

[a]yield & conversion are improved due to a increase in back pressure using the static mixer

(C) Real-time inline FT-IR reaction profile

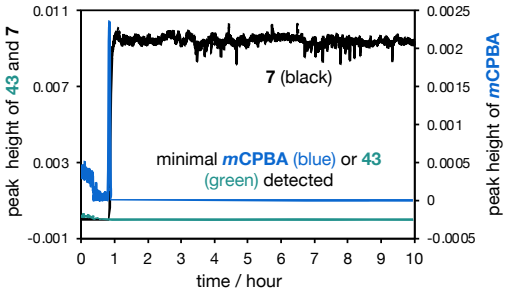

Figure 2. (A) Schematic of the continuous flow setup for preparative-scale synthesis. (B) Reaction optimization. (C) FT-IR reaction monitoring.

Finally, we demonstrated the potential of this method as an alternative to the most frequently employed [Ru]/$NaIO_4$ system in preparative-scale applications in process chemistry and total synthesis. We chose to investigate the scalability of the oxidation of carbamate **43** using commercially available ketoABNO (≈ 6 $/g).[52] First, process safety assessment was performed in a batch reactor (see SI). The reaction reached full conversion in 2 h at 25 ˚C with quantitative yield. While the reaction was substantially faster at 40 ˚C (full conversion in *ca.* 25 min), a lower yield (87%) was obtained and a rapid temperature spike to 70 ˚C was recorded. Indeed, calorimetry measurement showed the reaction has a reaction enthalpy (ΔH) of 180 kcal/mol and an adiabatic temperature increase was estimated to be 107 ˚C. To maintain fast reaction rate while addressing selectivity and safety challenges encountered with the batch reactor, we further developed a continuous flow process using a Corning G1 glass chip type reactor together with a static mixing unit (Figure 2A). A two-stream system was constructed followed by a MeOH quenching line, which served to dissolve *m*CBA byproduct. Upon optimization, 100% conversion was achieved in a short residence time of 15 min at a temperature of 48 ˚C. Solution temperature at the exit was stable and matched that of the blank solvent. Real-time FT-IR monitoring at the exit showed that the conversion and yield were consistent over the course of reaction and the residue *m*CPBA remained minimum. Overall, a continuous flow run of 544 min processed 93.8 g of amide **43** and produced desired **7** in average 94% assay yield.

In summary, we developed an oxoammonium-catalyzed chemoselective oxidation of *N*-substituted amines, which exhibits a broad substrate scope and can be readily scaled using continuous flow. This reaction undergoes a hydride transfer mechanism, which remains underexplored in C–H functionalization but provides complementary reactivity and selectivity to widely established radical-based approaches.

AUTHOR INFORMATION

Corresponding Author

Song Lin – Department of Chemistry and Chemical Biology, Cornell University, Ithaca, New York 14853, United States; orcid.org/0000-0002-8880-6476; Email: songlin@cornell.edu.

Authors

Jonas Rein – Department of Chemistry and Chemical Biology, Cornell University, Ithaca, New York 14853, United States; orcid.org/0000-0001-8237-6519.

Bartosz Górski – Department of Chemistry and Chemical Biology, Cornell University, Ithaca, New York 14853, United States; orcid.org/0000-0003-4644-9789.

Yukun Cheng – Department of Chemistry and Chemical Biology, Cornell University, Ithaca, New York 14853, United States; orcid.org/0000-0002-2379-9404.

Zhen Lei – Chemical Development U.S., Boehringer Ingelheim Pharmaceuticals, Inc., 900 Ridgebury Rd, Ridgefield, CT 06877, United States; orcid.org/0000-0002-6608-7933.

Frederic Buono – Chemical Development U.S., Boehringer Ingelheim Pharmaceuticals, Inc., 900 Ridgebury Rd, Ridgefield, CT 06877, United States; orcid.org/0000-0001-7585-0438.

Author Contributions

‡J. R. and B. G. contributed equally. †Y. C. and Z. L. contributed equally. The manuscript was written through contributions of all authors.

ACKNOWLEDGMENT

The research was supported by NIH (R01 GM134088) and Boehringer Ingelheim Pharmaceuticals, Inc. S.L. is grateful to the Dreyfus Foundation for a Teacher-Scholar Award. NMR data were collected on spectrometers that were purchased with support from the National Science Foundation (CHE-1531632). Buried volume analyses were performed with UCSF ChimeraX, developed by the Resource for Biocomputing, Visualization, and Informatics at the University of California, San Francisco, with support from National Institutes of Health R01-GM129325 and the Office of Cyber Infrastructure and Computational Biology, National Institute of Allergy and Infectious Diseases. We thank Samson B. Zacate for the

https://doi.org/10.26434/chemrxiv-2024-brd62 **ORCID:** https://orcid.org/0000-0001-8237-6519 Content not peer-reviewed by ChemRxiv. **License:** CC BY-NC 4.0

first synthesis of catalyst **A20**; Elya Kandahari for helpful discussions; Dr. Yi Wang for reaction reproduction.

REFERENCES

(1) Murahashi, S.-I.; Komiya, N. Ruthenium-Catalyzed Oxidation for Organic Synthesis. In *Modern Oxidation Methods*; John Wiley & Sons, Ltd, 2010; pp 241–275. https://doi.org/10.1002/9783527632039.ch7.

(2) Arends, I. W. C. E.; Kodama, T.; Sheldon, R. A. Oxidation Using Ruthenium Catalysts. In *Ruthenium Catalysts and Fine Chemistry*; Springer: Berlin, Heidelberg, 2004; pp 277–320. https://doi.org/10.1007/b94652.

(3) Finke, P. E.; Loebach, J. L.; Parker, K. A.; Plummer, C. W.; Mills, S. G. Cyclopentyl Modulators of Chemokine Receptor Activity. US7091211B2, August 15, 2006. https://patents.google.com/patent/US7091211B2/en (accessed 2024-07-12).

(4) CLAGG, K. B. P.; Gosselin, F.; Han, C.; KNIPPEL, J. L.; LUBACH, J.; Savage, S. Process for Preparing 1-Arylsulfonyl-Pyrrolidine-2-Carboxamide Transient Receptor Potential Channel Antagonist Compounds and Crystalline Forms Thereof. WO2019164778A1, August 29, 2019. https://patents.google.com/patent/WO2019164778A1/en (accessed 2024-07-12).

(5) Rakshit, S.; Sathasivam, S.; Reddy, R.; Rao, S. V.; Shekarappa, V.; Kandasamy, M.; Jaleel, M.; Murugan, S.; Bhat, A.; Subramani, T.; Lakshminarasimhan, T.; Gangu, A.; Wisniewski, S. R.; Kopp, N.; Hale, I.; Stevens, J. M.; Rosso, V. W.; Eastgate, M. D.; Vaidyanathan, R. Alternative Approach to the Large-Scale Synthesis of the Densely Functionalized Pyrrolidone BMT-415200. *Org. Process Res. Dev.* **2023**, *27* (4), 707–722. https://doi.org/10.1021/acs.oprd.3c00007.

(6) Donohoe, T. J.; O'Riordan, T. J. C.; Peifer, M.; Jones, C. R.; Miles, T. J. Asymmetric Synthesis of the Fully Elaborated Pyrrolidinone Core of Oxazolomycin A. *Org. Lett.* **2012**, *14* (21), 5460–5463. https://doi.org/10.1021/ol302541j.

(7) Umezawa, T.; Hayashi, T.; Sakai, H.; Teramoto, H.; Yoshikawa, T.; Izumida, M.; Tamatani, Y.; Hirose, T.; Ohfune, Y.; Shinada, T. Total Synthesis of (−)-5,6,11-Trideoxytetrodotoxin and Its 4-Epimer. *Org. Lett.* **2006**, *8* (21), 4971–4974. https://doi.org/10.1021/ol062098d.

(8) Amat, M.; Pinto, A.; Griera, R.; Bosch, J. Stereoselective Synthesis of (−)-Lepadins A–C. *Chem. Commun.* **2013**, *49* (94), 11032–11034. https://doi.org/10.1039/C3CC46801A.

(9) Varlet, T.; Portmann, S.; Fürstner, A. Total Synthesis of Njaoamine C by Concurrent Macrocycle Formation. *J. Am. Chem. Soc.* **2023**, *145* (39), 21197–21202. https://doi.org/10.1021/jacs.3c08410.

(10) Coutts, I. G. C.; Saint, R. E.; Saint, S. L.; Chambers-Asman, D. M. Homochiral 2-Aminoadipates and 6-Oxopipecolates From Glutamic Acid. *Synthesis* **2001**, *2001*, 247–250. https://doi.org/10.1055/s-2001-10814.

(11) Zhong, H.; Egger, D. T.; Gasser, V. C. M.; Finkelstein, P.; Keim, L.; Seidel, M. Z.; Trapp, N.; Morandi, B. Skeletal Metalation of Lactams through a Carbonyl-to-Nickel-Exchange Logic. *Nat Commun* **2023**, *14* (1), 5273. https://doi.org/10.1038/s41467-023-40979-3.

(12) Shaw, M. H.; Shurtleff, V. W.; Terrett, J. A.; Cuthbertson, J. D.; MacMillan, D. W. C. Native Functionality in Triple Catalytic Cross-Coupling: Sp3 C–H Bonds as Latent Nucleophiles. *Science* **2016**, *352* (6291), 1304–1308. https://doi.org/10.1126/science.aaf6635.

(13) Ahneman, D. T.; Doyle, A. G. C–H Functionalization of Amines with Aryl Halides by Nickel-Photoredox Catalysis. *Chem. Sci.* **2016**, *7* (12), 7002–7006. https://doi.org/10.1039/C6SC02815B.

(14) Vasilopoulos, A.; Krska, S. W.; Stahl, S. S. C(Sp3)–H Methylation Enabled by Peroxide Photosensitization and Ni-Mediated Radical Coupling. *Science* **2021**, *372* (6540), 398–403. https://doi.org/10.1126/science.abh2623.

(15) Frankowski, K. J.; Liu, R.; Milligan, G. L.; Moeller, K. D.; Aubé, J. Practical Electrochemical Anodic Oxidation of Polycyclic Lactams for Late Stage Functionalization. *Ang. Chem. Int. Ed.* **2015**, *54* (36), 10555–10558. https://doi.org/10.1002/anie.201504775.

(16) Novaes, L. F. T.; Ho, J. S. K.; Mao, K.; Liu, K.; Tanwar, M.; Neurock, M.; Villemure, E.; Terrett, J. A.; Lin, S. Exploring Electrochemical C(Sp3)–H Oxidation for the Late-Stage Methylation of Complex Molecules. *J. Am. Chem. Soc.* **2022**, *144* (3), 1187–1197. https://doi.org/10.1021/jacs.1c09412.

(17) Based on *Reaxys* and *Scifinder* serches accessed on June 20, 2024; see SI for a full account of oxidation conditions.

(18) Zhao, J.; Nanjo, T.; de Lucca, E. C.; White, M. C. Chemoselective Methylene Oxidation in Aromatic Molecules. *Nat. Chem* **2019**, *11* (3), 213–221. https://doi.org/10.1038/s41557-018-0175-8.

(19) Feng, K.; Quevedo, R. E.; Kohrt, J. T.; Oderinde, M. S.; Reilly, U.; White, M. C. Late-Stage Oxidative C(Sp3)–H Methylation. *Nature* **2020**, *580* (7805), 621–627. https://doi.org/10.1038/s41586-020-2137-8.

(20) Osberger, T. J.; Rogness, D. C.; Kohrt, J. T.; Stepan, A. F.; White, M. C. Oxidative Diversification of Amino Acids and Peptides by Small-Molecule Iron Catalysis. *Nature* **2016**, *537* (7619), 214–219. https://doi.org/10.1038/nature18941.

(21) Wang, F.; Rafiee, M.; Stahl, S. S. Electrochemical Functional-Group-Tolerant Shono-Type Oxidation of Cyclic Carbamates Enabled by Aminoxyl Mediators. *Angew. Chem. Int. Ed.* **2018**, *57* (22), 6686–6690. https://doi.org/10.1002/anie.201803539.

(22) Hamlin, T. A.; Kelly, C. B.; Ovian, J. M.; Wiles, R. J.; Tilley, L. J.; Leadbeater, N. E. Toward a Unified Mechanism for Oxoammonium Salt-Mediated Oxidation Reactions: A Theoretical and Experimental Study Using a Hydride Transfer Model. *J. Org. Chem.* **2015**, *80* (16), 8150–8167. https://doi.org/10.1021/acs.joc.5b01240.

(23) Richter, H.; García Mancheño, O. Dehydrogenative Functionalization of C(Sp3)–H Bonds Adjacent to a Heteroatom Mediated by Oxoammonium Salts. *Eur. J. Org. Chem.* **2010**, *2010* (23), 4460–4467. https://doi.org/10.1002/ejoc.201000548.

(24) Fang, L.; Li, Z.; Jiang, Z.; Tan, Z.; Xie, Y. A Metal-Free Oxidative Cross-Dehydrogenative Coupling of N-Aryl Tetrahydroisoquinolines and 2-Methylazaarenes Using a Recyclable Oxoammonium Salt as Oxidant in Aqueous Media. *Eur. J. Org. Chem.* **2016**, *2016* (21), 3559–3567. https://doi.org/10.1002/ejoc.201600423.

(25) Carlet, F.; Bertarini, G.; Broggini, G.; Pradal, A.; Poli, G. Oxoammonium-Mediated Allylsilane–Ether Coupling Reaction. *Eur. J. Org. Chem.* **2021**, *2021* (15), 2162–2168. https://doi.org/10.1002/ejoc.202100026.

(26) Miller, J. L.; Damodaran, K.; Floreancig, P. E. Nitrogen Heterocycle Synthesis through Hydride Abstraction of Acyclic Carbamates and Related Species: Scope, Mechanism, Stereoselectivity, and Product Conformation Studies. *Chem. Eur. J* **2023**, *29* (71), e202302977. https://doi.org/10.1002/chem.202302977.

(27) Nutting, J. E.; Rafiee, M.; Stahl, S. S. Tetramethylpiperidine N-Oxyl (TEMPO), Phthalimide N-Oxyl (PINO), and Related N-Oxyl Species: Electrochemical Properties and Their

https://doi.org/10.26434/chemrxiv-2024-brd62 **ORCID:** https://orcid.org/0000-0001-8237-6519 Content not peer-reviewed by ChemRxiv. **License:** CC BY-NC 4.0

Use in Electrocatalytic Reactions. *Chem. Rev.* **2018**, *118* (9), 4834–4885. https://doi.org/10.1021/acs.chemrev.7b00763.
(28) Nagasawa, S.; Sasano, Y.; Iwabuchi, Y. THE UTILITY OF OXOAMMONIUM SPECIES IN ORGANIC SYNTHESIS: BEYOND ALCOHOL OXIDATION. *Heterocycles* **2022**, *105* (1), 61–114. https://doi.org/10.3987/REV-21-SR(R)2.
(29) Deprez, N. R.; Clausen, D. J.; Yan, J.-X.; Peng, F.; Zhang, S.; Kong, J.; Bai, Y. Selective Electrochemical Oxidation of Functionalized Pyrrolidines. *Org. Lett.* **2021**, *23* (22), 8834–8837. https://doi.org/10.1021/acs.orglett.1c03338.
(30) Sabnis, R. W. Novel 5-Alkyl Pyrrolidine Orexin Receptor Agonists for Treating Sleep Disorders. *ACS Med. Chem. Lett.* **2020**, *11* (11), 2085–2086. https://doi.org/10.1021/acsmedchemlett.0c00501.
(31) Nagasawa, S.; Sasano, Y.; Iwabuchi, Y. Catalytic Oxygenative Allylic Transposition of Alkenes into Enones with an Azaadamantane-Type Oxoammonium Salt Catalyst. *Eur. J. Org. Chem.* **2017**, *23* (43), 10276–10279. https://doi.org/10.1002/chem.201702512.
(32) Inokuchi, T.; Kawafuchi, H. Reactivity of TEMPO Anion as a Nucleophile and Its Applications for Selective Transformations of Haloalkanes or Acyl Halides to Aldehydes. *Tetrahedron* **2004**, *60* (51), 11969–11975. https://doi.org/10.1016/j.tet.2004.09.067.
(33) Smaligo, A. J.; Wu, J.; Burton, N. R.; Hacker, A. S.; Shaikh, A. C.; Quintana, J. C.; Wang, R.; Xie, C.; Kwon, O. Oxodealkenylative Cleavage of Alkene C(Sp3)−C(Sp2) Bonds: A Practical Method for Introducing Carbonyls into Chiral Pool Materials. *Angew. Chem. Int. Ed.* **2020**, *59* (3), 1211–1215. https://doi.org/10.1002/anie.201913201.
(34) Rafiee, M.; Miles, K. C.; Stahl, S. S. Electrocatalytic Alcohol Oxidation with TEMPO and Bicyclic Nitroxyl Derivatives: Driving Force Trumps Steric Effects. *J. Am. Chem. Soc.* **2015**, *137* (46), 14751–14757. https://doi.org/10.1021/jacs.5b09672.
(35) Hickey, D. P.; Schiedler, D. A.; Matanovic, I.; Doan, P. V.; Atanassov, P.; Minteer, S. D.; Sigman, M. S. Predicting Electrocatalytic Properties: Modeling Structure–Activity Relationships of Nitroxyl Radicals. *J. Am. Chem. Soc.* **2015**, *137* (51), 16179–16186. https://doi.org/10.1021/jacs.5b11252.
(36) Falivene, L.; Credendino, R.; Poater, A.; Petta, A.; Serra, L.; Oliva, R.; Scarano, V.; Cavallo, L. SambVca 2. A Web Tool for Analyzing Catalytic Pockets with Topographic Steric Maps. *Organometallics* **2016**, *35* (13), 2286–2293. https://doi.org/10.1021/acs.organomet.6b00371.
(37) Schaefer, A. J.; Ingman, V. M.; Wheeler, S. E. SEQCROW: A ChimeraX Bundle to Facilitate Quantum Chemical Applications to Complex Molecular Systems. *J. Comput. Chem.* **2021**, *42* (24), 1750–1754. https://doi.org/10.1002/jcc.26700.
(38) Shibuya, M.; Pichierri, F.; Tomizawa, M.; Nagasawa, S.; Suzuki, I.; Iwabuchi, Y. Oxidation of Nitroxyl Radicals: Electrochemical and Computational Studies. *Tetrahedron Lett.* **2012**, *53* (16), 2070–2073. https://doi.org/10.1016/j.tetlet.2012.02.033.
(39) Shibuya, M.; Osada, Y.; Sasano, Y.; Tomizawa, M.; Iwabuchi, Y. Highly Efficient, Organocatalytic Aerobic Alcohol Oxidation. *J. Am. Chem. Soc.* **2011**, *133* (17), 6497–6500. https://doi.org/10.1021/ja110940c.
(40) Shibuya, M.; Nagasawa, S.; Osada, Y.; Iwabuchi, Y. Mechanistic Insight into Aerobic Alcohol Oxidation Using NOx–Nitroxide Catalysis Based on Catalyst Structure–Activity Relationships. *J. Org. Chem.* **2014**, *79* (21), 10256–10268. https://doi.org/10.1021/jo501862k.
(41) Lauber, M. B.; Stahl, S. S. Efficient Aerobic Oxidation of Secondary Alcohols at Ambient Temperature with an ABNO/NOx Catalyst System. *ACS Catal.* **2013**, *3* (11), 2612–2616. https://doi.org/10.1021/cs400746m.
(42) Gerken, J. B.; Pang, Y. Q.; Lauber, M. B.; Stahl, S. S. Structural Effects on the pH-Dependent Redox Properties of Organic Nitroxyls: Pourbaix Diagrams for TEMPO, ABNO, and Three TEMPO Analogs. *J. Org. Chem.* **2018**, *83* (14), 7323–7330. https://doi.org/10.1021/acs.joc.7b02547.
(43) Cheng, Y.; Rein, J.; Le, N.; Lin, S. Oxoammonium-Catalyzed Ether Oxidation via Hydride Abstraction: Methodology Development and Mechanistic Investigation Using Paramagnetic Relaxation Enhancement NMR. *ChemRxiv* **2024**.
(44) This is supported by the comparison of the cyclic voltammograms of ketoABNO (**A4**) in MeCN and DCE showing that the oxoammonium cation is +46 mV more oxidizing in DCE when compared to a ferrocenium/ferrocene reference.
(45) Katoh, M.; Matsune, R.; Nagase, H.; Honda, T. Stereocontrolled Synthesis of a Potent Antimalarial Alkaloid, (+)-Febrifugine. *Tetrahedron Lett.* **2004**, *45* (33), 6221–6223. https://doi.org/10.1016/j.tetlet.2004.06.100.
(46) Dhudshia, B.; Cooper, B. F. T.; Macdonald, C. L. B.; Thadani, A. N. The Asymmetric Total Synthesis of (−)-Securinine. *Chem. Commun.* **2009**, No. 4, 463–465. https://doi.org/10.1039/B816576A.
(47) Chirkin, E.; Bouzidi, C.; Porée, F.-H. Tungsten-Promoted Hetero-Pauson–Khand Cycloaddition: Application to the Total Synthesis of (–)-Allosecurinine. *Synthesis* **2019**, *51*, 2001–2006. https://doi.org/10.1055/s-0037-1612063.
(48) Gao, B.; Chen, S.; Nan Hou, Y.; Juan Zhao, Y.; Ye, T.; Xu, Z. Solution-Phase Total Synthesis of Teixobactin. *Org. Biomol. Chem.* **2019**, *17* (5), 1141–1153. https://doi.org/10.1039/C8OB02803F.
(49) A full account of all other attempted substrates including suboptimal and unsuccessful ones are provided in the supporting information.
(50) Zhang, Y.; Zhang, T.; Das, S. Selective Functionalization of Benzylic C(Sp3)–H Bonds to Synthesize Complex Molecules. *Chem* **2022**, *8* (12), 3175–3201. https://doi.org/10.1016/j.chempr.2022.10.005.
(51) Kasai, M.; Ziffer, H. Ruthenium Tetroxide Catalyzed Oxidations of Aromatic and Heteroaromatic Rings. *J. Org. Chem.* **1983**, *48* (14), 2346–2349. https://doi.org/10.1021/jo00162a009.
(52) ketoABNO (CAS No.: 7123-92-4) was purchased from PharmaBlock (PBU1333). Pricing data was accessed on Aug. 22, 2024.

https://doi.org/10.26434/chemrxiv-2024-brd62 **ORCID:** https://orcid.org/0000-0001-8237-6519 Content not peer-reviewed by ChemRxiv. **License:** CC BY-NC 4.0

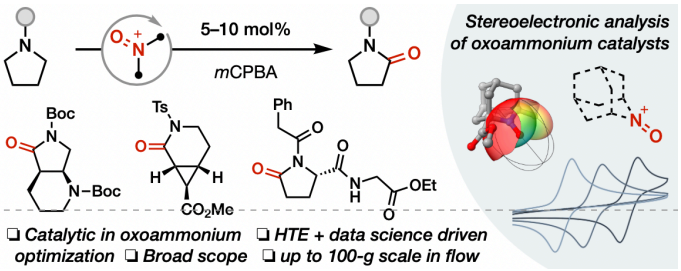

https://doi.org/10.26434/chemrxiv-2024-brd62 **ORCID:** https://orcid.org/0000-0001-8237-6519 Content not peer-reviewed by ChemRxiv. **License:** CC BY-NC 4.0